



# Combined Pressure Sensor With Enhanced Dynamic Range Based on Thin Films of Nanotubes and Graphite Nanobelts

Andrei Alaferdov<sup>1,2\*</sup>, Ilya Vilkov<sup>3</sup>, Boris Kaverin<sup>3</sup>, Anatoly Ob'edkov<sup>3</sup> and Stanislav Moshkalev<sup>1\*</sup>

<sup>1</sup>Center for Semiconductor Components and Nanotechnologies, University of Campinas, Campinas, Brazil, <sup>2</sup>Department of Applied Physics, The "Gleb Wataghin" Institute of Physics, University of Campinas, Campinas, Brazil, <sup>3</sup>Laboratory of Hybrid Nanomaterials, G. A. Razuvaev Institute of Organometallic Chemistry of Russian Academy of Sciences, Nizhny Novgorod, Russia

## OPEN ACCESS

### Edited by:

He Tian,  
Tsinghua University, China

### Reviewed by:

Yanhua Luo,  
University of New South Wales,  
Australia  
Zegao Wang,  
Sichuan University, China  
Xing Wu,  
East China Normal University, China  
Lu-Qi Tao,  
Chongqing University, China

### \*Correspondence:

Andrei Alaferdov  
analaferdov@gmail.com  
Stanislav Moshkalev  
stanisla@unicamp.br

### Specialty section:

This article was submitted to  
Physical Sensors,  
a section of the journal  
Frontiers in Sensors

**Received:** 15 October 2020

**Accepted:** 21 December 2020

**Published:** 27 January 2021

### Citation:

Alaferdov A, Vilkov I, Kaverin B,  
Ob'edkov A and Moshkalev S (2021)  
Combined Pressure Sensor With  
Enhanced Dynamic Range Based on  
Thin Films of Nanotubes and  
Graphite Nanobelts.  
Front. Sens. 1:617805.  
doi: 10.3389/fsens.2020.617805

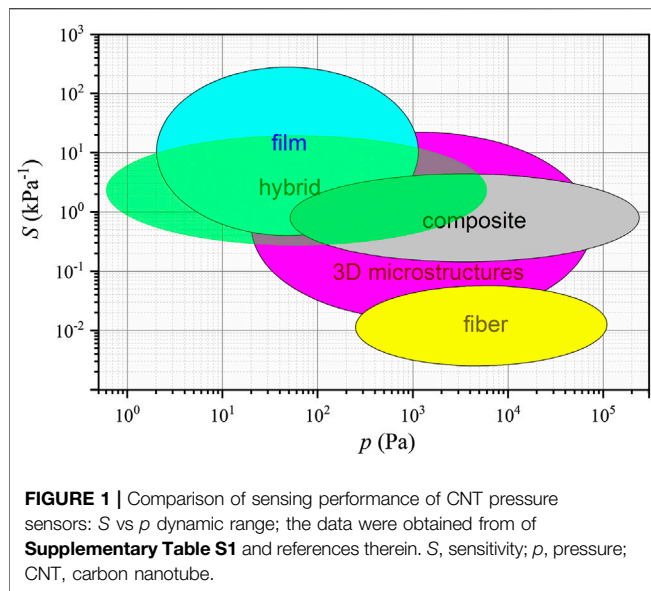
Herein, we demonstrate the prototype of a combined flexible pressure sensor based on ultrathin multiwall carbon nanotubes (MWCNTs) and graphite nanobelts (GNBs) films embedded in polydimethylsiloxane (PDMS). A simple and scalable modified Langmuir–Blodgett method was used for deposition of both MWCNT and GNB films. The use of two types of carbon nanostructures (nanotubes and GNBs) with distinctly different mechanical properties allowed obtaining enhanced dynamic range for pressure sensing. Short response time, good sensibility and flexibility, and low power consumption for enhanced pressure range make possible applications of the sensor for healthcare monitoring and as a component in the human–machine interfaces application.

**Keywords:** pressure sensor, multiwall carbon nanotubes, graphite nanobelts, Langmuir-Blodgett, thin flexible films

## INTRODUCTION

Novel flexible and wearable electronic devices have attracted much interest in the last decade, with numerous applications that span from simple recreational exercise monitoring to rare heart disease diagnostics, human sensory capabilities, and soft robotics (Kim et al., 2011). For development of flexible sensors, integration of sensing materials with flexible substrates and elements for signal processing is highly required.

Low fabrication cost, chemical and thermal stability, easy manipulation, and transfer onto different types of substrates make carbon nanostructure (CNS) materials (such as multilayer graphene or nanographite flakes and carbon nanotubes (CNTs)) highly suitable for flexible electronics (Obiedkov et al., 2012; Alaferdov et al., 2014; Wang et al., 2019; Zheng et al., 2020). Sensors based on these materials as building blocks showed high sensitivity and reproducibility for strain, pressure, and physiological signals monitoring (Sun et al., 2015; Wang et al., 2019). CNTs in different arrangements (thin and thick films, composites, hybrids, fibers, etc.) are widely used in pressure sensor fabrication (**Figure 1**), with the choice of the sensor configuration depending on the specific application. In particular, CNT-based pressure sensors with 3D microstructured architecture (Ul Hasan et al., 2016; Li et al., 2017; Zhan et al., 2017; Chen et al., 2020), in hybrid materials (Jian et al., 2017; Ma et al., 2020) or composites (Lee et al., 2016; Zhuang et al., 2020) demonstrate wide dynamic range but are characterized by a relatively complex process of fabrication. Sensors with CNT-composed fibers (Tai and Lubineau, 2016; Han et al., 2020) usually work at higher pressures and are characterized by reduced sensitivity. Thin films (Wang et al., 2014; Park et al., 2018) of



nanotubes demonstrate high sensitivity but relatively low dynamic range and higher limit of sensing. Sensors based on multilayer graphene or nanographite (Alaferdov et al., 2017) can be used for monitoring of higher pressures. In this way, usually one type of graphite nanostructure is used for pressure sensor fabrication. This leads to low dynamic range, reduced sensitivity, or response/recovery time and is frequently characterized by the complex procedure of fabrication. Thus, it motivated us to create a pressure sensor with a wide dynamic range using simple and low-cost techniques of fabrication, which also demonstrates short enough recovery/response time and sensitive to detect several types of signals.

In this work, we present the prototype of a thin, flexible, and wearable piezoresistive pressure sensor composed of two sensitive elements—MWCNTs and GNBs films embedded in PDMS layers—which can be integrated into one device with low power consumption (up to a few mW) and enhanced dynamic range. Specifically, thin semitransparent MWCNTs films exhibit high sensitivity in the low-pressure region (up to 200 Pa), and thin opaque GNBs films can be used as a sensitive element for pressures between 200 Pa and 10 kPa. The reliable, simple, low-cost, and scalable modified Langmuir–Blodgett (LB) method was used for deposition of both types of films. Wide dynamic range and short response/recovery time of the device make this kind of combined pressure sensors very promising applications in medical health monitoring, wearable electronics, human–computer interaction, and bionic prosthetics.

## MATERIALS AND METHODS

### Materials

MWCNTs with ~50 nm diameter (supplied by G.A. Razuvaev Institute of Organometallic Chemistry, Russia) were synthesized by the MOCVD method using ferrocene and toluene as

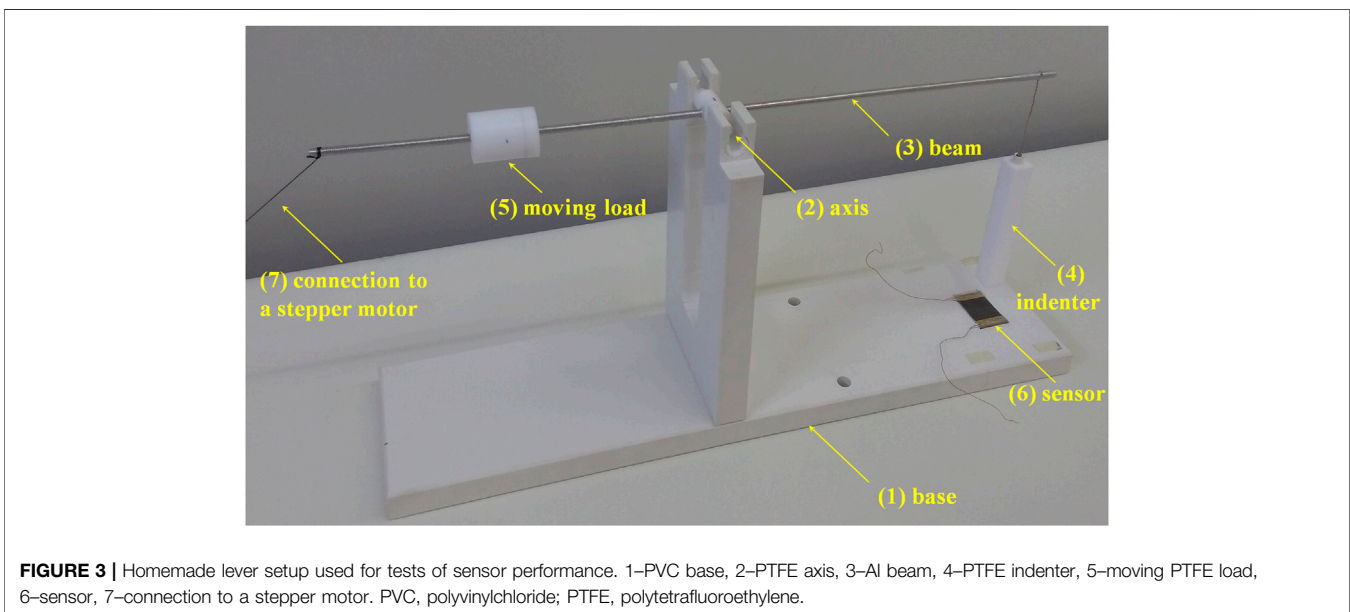
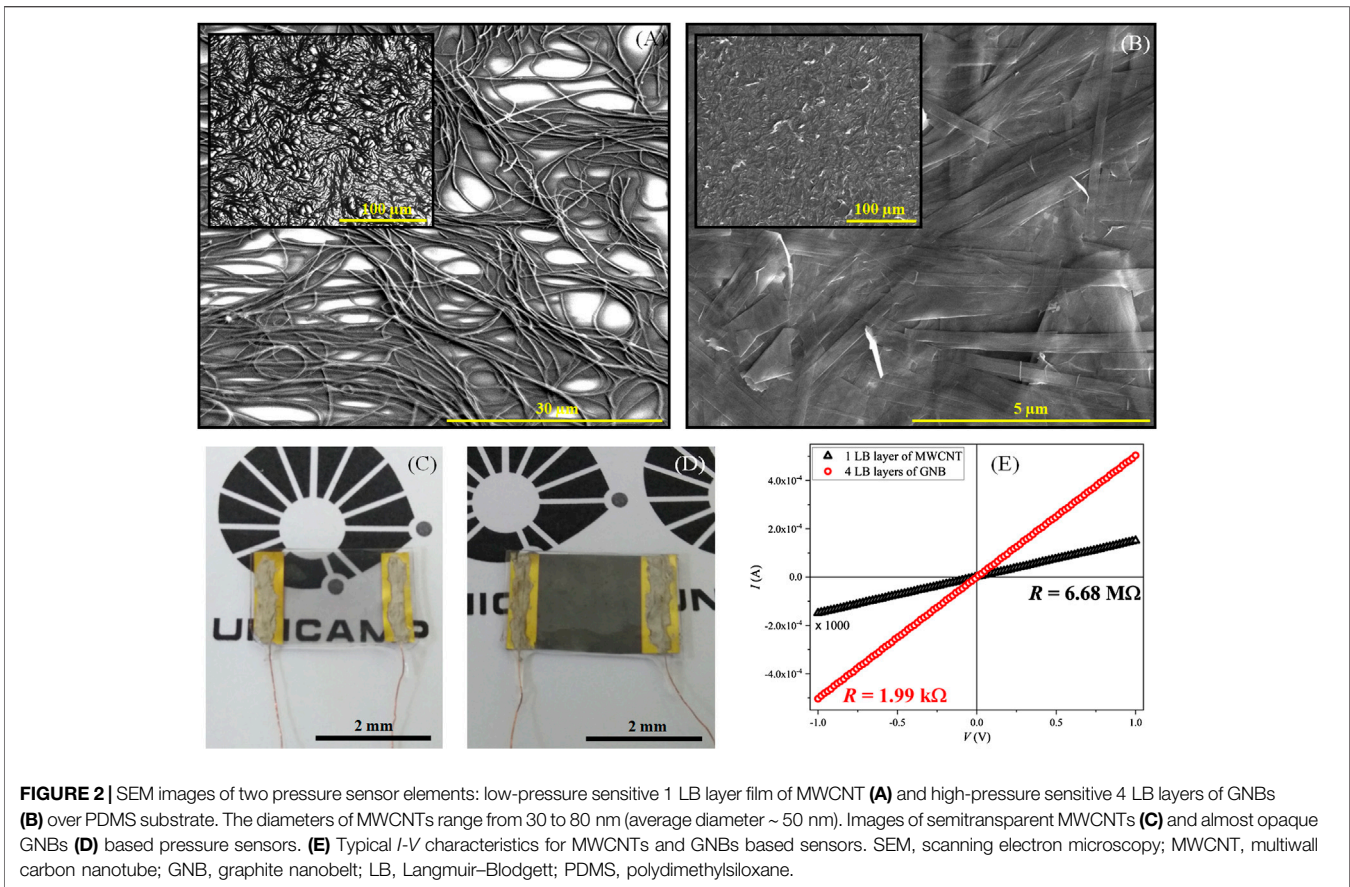
precursors (Obiedkov et al., 2012). GNBs (supplied by Nacional de Grafite Ltda, Brazil) were obtained from natural graphite by liquid-phase chemically assisted exfoliation technique (Hernandez et al., 2008; Alaferdov et al., 2014). Flexible, transparent, and biocompatible PDMS sheets were used as substrate and covered layers for the sensor fabrication. For substrates, commercial elastomeric PDMS sheets, with a thickness of 250  $\mu\text{m}$ , were used (Bisco® HT-6240, Rogers Corp.). To fabricate a top protective layer with thickness near 150  $\mu\text{m}$ , PDMS in the liquid form was used (Sylgard 184, Dow Corning Corporation).

To analyze the morphology structure of sensitive films deposited by the LB method, scanning electron microscopy (SEM; Nova 200 Nanolab, FEI) was performed. The crystalline quality of CNSs was investigated by micro-Raman spectroscopy (NT-MDT NTEGRA Spectra, with a 473 nm laser).

### Sensor Fabrication and Characterization

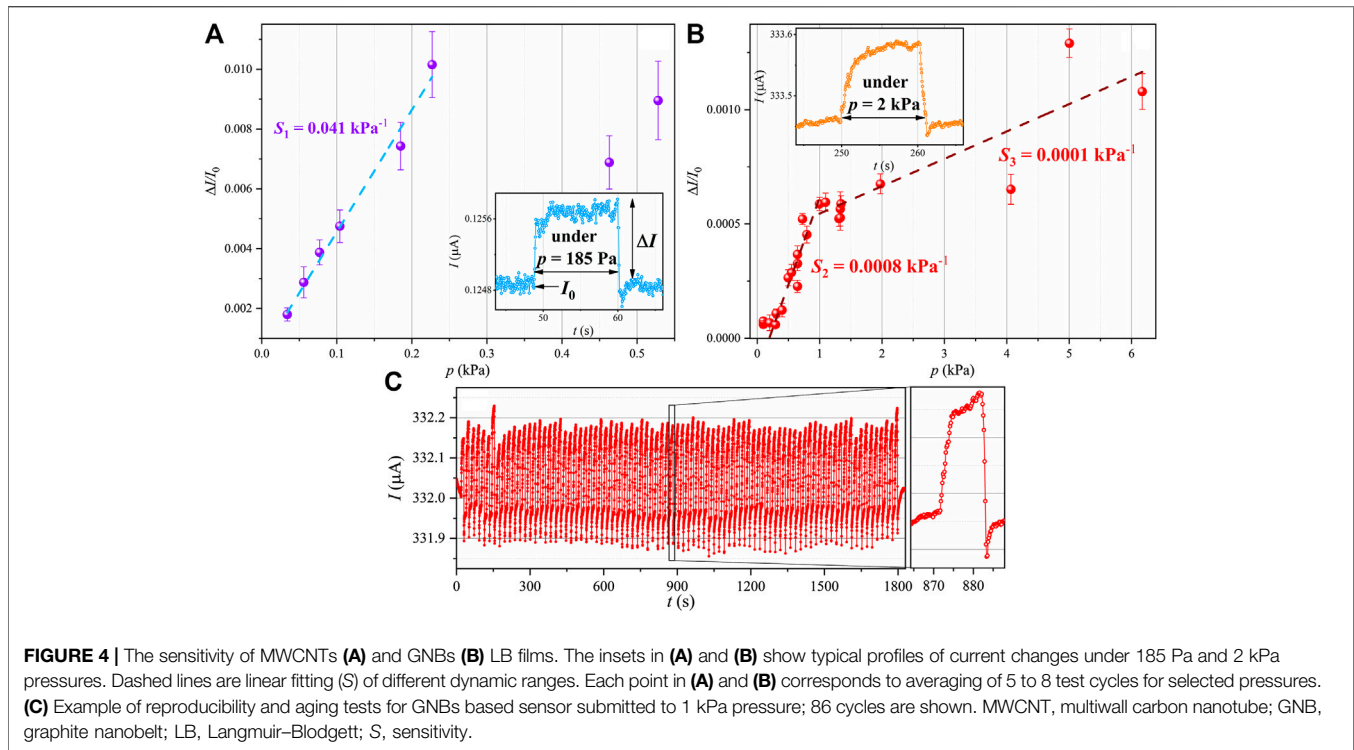
For films deposition, MWCNTs or GNBs powders were dispersed in N-Methyl-2-pyrrolidone solution at concentrations 0.2 mg/ml and 0.5 mg/ml, respectively, using an ultrasonic bath (Unique USC-1880, 100 W, 37 kHz). Then, using 1 ml of GNBs or 1 ml of MWCNTs suspensions, nanofilms were deposited onto 100  $\times$  45 mm solid flexible PDMS substrates by the modified LB method (see for details Alaferdov et al., 2016) using a homemade trapezoidal polytetrafluoroethylene (PTFE) cuvette filled with deionized water; after careful distribution of the suspension by a microsyringe over the water surface, the formation of a compact CNS (nanotubes or nanobelts) film occurs by draining water slowly through a hole at the cuvette's bottom and thus reducing the water surface area due to the cuvette shape. As the water level goes down, the compacted CNS film is transferred onto the PDMS fixed on the lower part of the vertically oriented cuvette wall; this wall is opposite to the one inclined at an angle of 45°. Before film depositions, the PDMS surface was treated by atmospheric pressure plasma (Nascimento et al., 2016), resulting in the decrease of PDMS surface roughness (mean roughness decreased by an order of magnitude, from ~40 nm down to 5 nm) and the increase of CNS film adhesion to the surface. The procedure of film deposition was repeated 4 times (followed by 4 h drying at normal condition after each deposition) in the case of GNBs. A high degree of crystallinity was proved by Raman measurements for both GNBs and MWCNTs films (**Supplementary Figure S1**, see detailed characterization in (Obiedkov et al., 2012; Alaferdov et al., 2018, 2020)).

The as-obtained films formed by randomly oriented percolated nanotubes (**Figure 2A**) or nanobelts (**Figure 2B**) are quite uniform. Since the PDMS surface is not flat, films do not cover completely its surface, leaving some areas uncovered and thus semitransparent after the first deposition (**Figure 1A**). Next, 15  $\times$  25 mm pieces of films were cut, and 5 mm width metallic Ti (30 nm)/Au (200 nm) contact electrodes were deposited by sputtering at two opposite edges of the films using a shadow mask. Finally, Cu metallic wires were connected to electrodes using conducting epoxy paste, and



the structure was packed using liquid PDMS (thermally cured at 90°C for 1 h), achieving total a device thickness of about 400 μm (**Figure 2C,D**). Electrical measurements were

performed to confirm ohmic behavior in both types of sensors, with typical resistance of a few kΩ for GNB-based sensor and a few MΩ for films of MWCNT (**Figure 2E**).



## Sensor Testing

The sensor tests have been carried out using a homemade lever setup (**Figure 3**) developed to provide pressures with fine adjustment in a wide range between 30 Pa and 10 kPa. The measurements of the pressure impact on the sensor (6) fixed on the base (1) were realized using standard torque equation for two bodies localized on a rigid Al beam (3) supported on a PTFE axis (2); the fixed  $1 \times 1$  cm cross-section PTFE indenter (4) and moving PTFE load (5). The pressure applied by the indenter on a sample surface depends on moving load position. In this way, necessary pressure determined by equation for left beam was obtained from the torque equation for two bodies:

$$l_2 = \frac{l_1}{m_2 g} (m_1 g - pS),$$

where  $l_2$  is the distance between the load and axis position;  $l_1$  is the distance between the indenter and axis position;  $m_1$  and  $m_2$  are masses of the indenter and load, respectively;  $S$  is the indenter cross-section;  $p$  is the pressure applied to the sample surface; and  $g$  is standard gravity. The changes of electrical current in load/unload states were measured using a B2912A Agilent source-meter by applying a constant voltage of 1 V. The measurement process for cycling pressure was automatized using a stepper motor connected to one end of the beam (7).

## RESULTS

The measurements were performed to show the current changes under applied pressure (see **Figure 4** and insets in it). Detailed

**TABLE 1 |** Estimated characteristic response and recovery times for two types of sensors at different pressures.

Sensor type	MWCNTs		GNBs	
$p$ (Pa)	34	185	549	6,171
$t_{res}$ (s)	0.37	0.16	1.03	0.13
$t_{rec}$ (s)	0.20	0.13	0.55	0.48

MWCNT, multiwall carbon nanotube; GNB, graphite nanobelt.

analysis of the response temporal behavior was done to estimate the characteristic response ( $t_{res}$ ) and recovery ( $t_{rec}$ ) times at different pressures (**Table 1**). It was found that response as well as recovery time<sup>1</sup> usually have a magnitude of a few hundreds of ms that is sufficient for monitoring human physiological signals and applying in human–machine interfaces. Moreover, the decrease of both times was observed with pressure increase. It also should be noted that  $t_{rec}$  is superior to  $t_{res}$  at high pressures, whereas at low and moderate pressures, the recovery time is shorter than the response time.

Investigation of relative current changes under different pressures ( $\Delta I/I_0$ ) ( $p$ ) allowed to identify several specific regions for each type of sensors, characterized by different sensitivity calculated as  $S = (\Delta I/I_0)/\Delta p$ , where  $\Delta I$  is the current change due to pressure impact,  $I_0$  is the initial current value, and  $\Delta p$  is the

<sup>1</sup>The characteristic response (recovery) time has been calculated as  $t_{res(rec)} = t_i \pm t\left(\frac{\Delta I}{\epsilon}\right)$ , where  $t_i$  is the initial time,  $\Delta I$  is current changes due to pressure impact, and  $t\left(\frac{\Delta I}{\epsilon}\right)$  is the time when  $\Delta I$  changes for  $1/\epsilon$  times. Signs “+” and “-” correspond to response and recovery times, respectively.

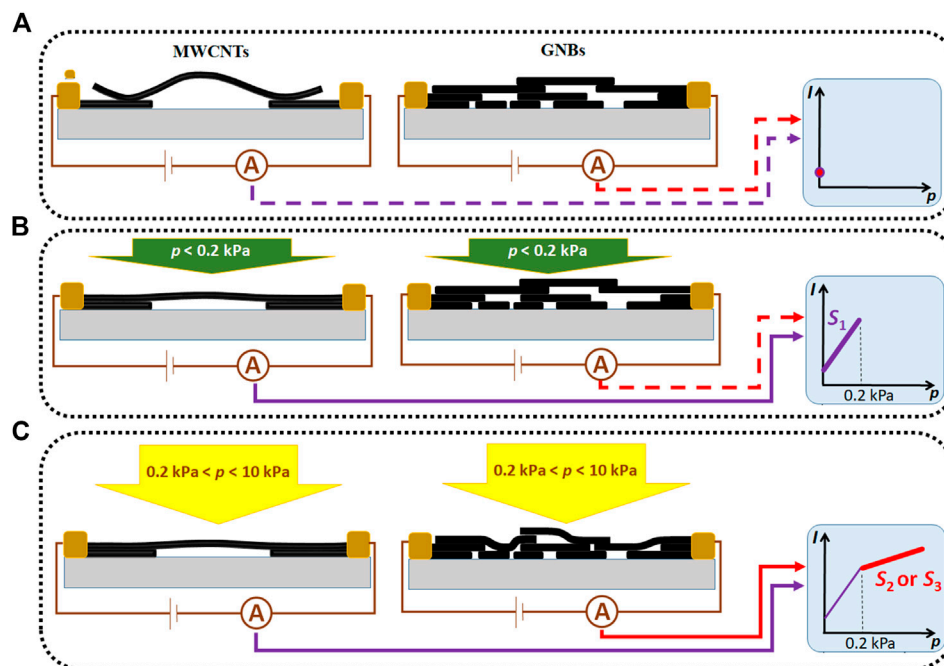


**FIGURE 5** | Schematic illustrations of the pressure sensing mechanism for combined sensor based on MWCNTs (left) and GNBs (right) films: **(A)** The initial relaxed state; **(B)** loaded state at pressures  $p < 0.2$  kPa, characterized by increasing contact areas between MWCNTs and corresponding fast current increase with pressure, while only small current changes are observed for GNBs film; **(C)** loaded state at pressures of  $0.2$  kPa  $< p < 10$  kPa, characterized by small changes of contact areas between MWCNTs and increasing contact areas between nanobelts. The sensor response to pressure is shown in the right images for each case. MWCNT, multiwall carbon nanotube; GNB, graphite nanobelt.

pressure change (Figure 4). A near linear dependence of response on pressure has been observed between 30 and 200 Pa regions for MWCNTs films (Figure 4A) and for two regions in the case of GNBs films: (i) between 200 Pa and 1 kPa and (ii) at  $p > 1$  kPa (Figure 4B). Notably, only weak changes of current are observed for pressures exceeding  $\sim 200$  Pa for the MWCNTs sensor and at pressures lower than 200 Pa for the GNBs sensor.

Cyclic tests performed on both types of sensors indicated good electromechanical stability and reversibility of devices (Figure 4C).

## DISCUSSION

The pressure-sensing mechanism in films is related to variations of contact areas between individual nanostructures resulting in current changes under applied pressure. Different mechanical properties of the films composed by nanotubes and GNBs (with the latter being more rigid and flat) provide sensitivities to different pressure ranges (larger pressures for more rigid nanobelts). Specifically, percolated nanotubes form point contacts between themselves in the LB film in a relaxed state (Figures 2A,5A). The low-pressure impact induces the flattening of initially curved nanotubes and fast rise of the contact areas, which results in fast current changes, i.e. high sensitivity. At the same time, the impact of low pressures is still negligible for more rigid GNBs films (Figure 5B). Further increase of pressure

evidently does not result in changes of contact areas for already compacted nanotubes films. Along with this, the gaps between individual nanobelts are reduced and areas of contacts between them start to increase with pressure, however, with much lower sensitivity (Figures 2B,5C). Further slower increase of the response at pressures higher than 1 kPa is probably due to deformations of supporting PDMS layers and related increase of contact areas between nanobelts. As the results, three distinct pressure regions are observed with decreasing sensitivities:  $S_1 > S_2 > S_3$ .

As nanotubes and nanobelts films demonstrate the ability to detect pressure impact in distinct pressure regions ( $S_1$  for nanotubes and  $S_2$ – $S_3$  for GNBs), these films can be integrated into one device and can act as combined sensitive elements in pressure sensors (Figure 5) with enhanced dynamic range and low power consumption, about 1 mW (estimated from Figure 2E). Taking into account the results of physiological signal-detecting tests obtained in our previous work in sensors contained only GNBs sensitive layer with reduced sensitivity and dynamic range (Alaferdov et al., 2017), the combined sensors developed in the current research can be employed for monitoring of cardiorespiratory signals, blood circulation in arteries, and breathing, with performance comparable with best results available in literature (Wang et al., 2014; Park et al., 2018) and MWCNTs (Jian et al., 2017).

Finally, in order to explore the lower limits of pressure detection (below 30 Pa) using the same sensor configuration,

the improvement of the test setup and sensor design is the subject of future work.

## CONCLUSIONS

In summary, we presented the prototype of a thin, flexible, biocompatible pressure sensor based on combined MWCNTs and GNBs films with an enhanced sensing range. Simple fabrication technique, biocompatibility of materials and low power consumption make our device a good choice for numerous biomedical applications.

## DATA AVAILABILITY STATEMENT

The raw data supporting the conclusions of this article will be made available by the authors, without undue reservation.

## AUTHOR CONTRIBUTIONS

AA and SM designed all experiments and characterizations. AA realized sensor fabrication procedure, characterization, and all electrical measurements. IV, BK, and AO synthesized the MWCNTs and participated in writing the manuscript. AA and

SM discussed the results of experiments and characterization of samples, proposed the models, organized data, and wrote the manuscript.

## FUNDING

This work has been supported by the São Paulo Research Foundation (FAPESP), process No. 2018/21623-0; the National Council for Scientific and Technological Development (CNPq); and the Russian Foundation for Basic Research (RFFI), grant No. 18-29-19137\_mk.

## ACKNOWLEDGMENTS

AA and SM thank the CCSNano/UNICAMP staff for technical assistance, especially MS Mara Canesqui for performing Raman measurements and Raluca Savu for sputtering deposition.

## SUPPLEMENTARY MATERIAL

The Supplementary Material for this article can be found online at: <https://www.frontiersin.org/articles/10.3389/fsens.2020.617805/full#supplementary-material>.

## REFERENCES

- Alaferdov, A. V., Savu, R., Fantini, C., Caçado, L. G., Moshkalev, S. A., and Moshkalev, S. A. (2020). Raman spectra of multilayer graphene under high temperatures. *J. Phys. Condens. Matter* 32, 385704. doi:10.1088/1361-648X/ab95ce
- Alaferdov, A. V., Savu, R., Rackauskas, T. A., Rackauskas, S., Canesqui, M. A., de Lara, D. S., et al. (2016). A wearable, highly stable, strain and bending sensor based on high aspect ratio graphite nanobelts. *Nanotechnology* 27, 375501. doi:10.1088/0957-4484/27/37/375501
- Alaferdov, A. V., Gholamipour-Shirazi, A., Canesqui, M. A., Danilov, Y. A., and Moshkalev, S. A. (2014). Size-controlled synthesis of graphite nanoflakes and multi-layer graphene by liquid phase exfoliation of natural graphite. *Carbon N. Y.* 69, 525–535. doi:10.1016/j.carbon.2013.12.062
- Alaferdov, A. V., Savu, R., Canesqui, M. A., Bortolucci, E., Joanni, E., Peressinoto, J., et al. (2017). Graphite nanobelts characterization and application for blood pulse sensing. *Int. J. Metrol. Qual. Eng.* 8, 6. doi:10.1051/ijmqe/2017003
- Alaferdov, A. V., Savu, R., Canesqui, M. A., Kopelevich, Y. V., da Silva, R. R., Rozhkova, N. N., et al. (2018). Ripplcation in graphite nanoplatelets during sonication assisted liquid phase exfoliation. *Carbon N. Y.* 129, 826–829. doi:10.1016/j.carbon.2017.12.100
- Ul Hasan, S. A., Jung, Y., Kim, S., Jung, C. L., Oh, S., Kim, J., et al. (2016). A sensitivity enhanced MWCNT/PDMS tactile sensor using micropillars and low energy Ar<sup>+</sup> ion beam treatment. *Sensors* 16, 93. doi:10.3390/s16010093
- Chen, X., Lin, X., Mo, D., Xia, X., Gong, M., Lian, H., et al. (2020). High-sensitivity, fast-response flexible pressure sensor for electronic skin using direct writing printing. *RSC Adv.* 10, 26188–26196. doi:10.1039/D0RA04431H
- Han, M., Lee, J., Kim, J. K., An, H. K., Kang, S. W., and Jung, D. (2020). Highly sensitive and flexible wearable pressure sensor with dielectric elastomer and carbon nanotube electrodes. *Sensors Actuators A Phys.* 305, 111941. doi:10.1016/j.sna.2020.111941
- Hernandez, Y., Nicolosi, V., Lotya, M., Blighe, F. M., Sun, Z., De, S., et al. (2008). High-yield production of graphene by liquid-phase exfoliation of graphite. *Nat. Nanotechnol.* 3, 563–568. doi:10.1038/nnano.2008.215
- Jian, M., Xia, K., Wang, Q., Yin, Z., Wang, H., Wang, C., et al. (2017). Flexible and highly sensitive pressure sensors based on bionic hierarchical structures. *Adv. Funct. Mater.* 27, 1606066. doi:10.1002/adfm.201606066
- Kim, D. H., Lu, N., Ma, R., Kim, Y. S., Kim, R. H., Wang, S., et al. (2011). Epidermal electronics. *Science* 333, 838–843. doi:10.1126/science.1206157
- Lee, S., Reuveny, A., Reeder, J., Lee, S., Jin, H., Liu, Q., et al. (2016). A transparent bending-insensitive pressure sensor. *Nat. Nanotechnol.* 11, 472–478. doi:10.1038/nnano.2015.324
- Li, X., Huang, W., Yao, G., Gao, M., Wei, X., Liu, Z., et al. (2017). Highly sensitive flexible tactile sensors based on microstructured multiwall carbon nanotube arrays. *Scripta Mater.* 129, 61–64. doi:10.1016/j.scriptamat.2016.10.037
- Ma, Z., Wang, W., and Yu, D. (2020). Highly sensitive and flexible pressure sensor prepared by simple printing used for micro motion detection. *Adv. Mater. Interfaces* 7, 1–7. doi:10.1002/admi.201901704
- Nascimento, F., Parada, S., Moshkalev, S., and Machida, M. (2016). Plasma treatment of poly(dimethylsiloxane) surfaces using a compact atmospheric pressure dielectric barrier discharge device for adhesion improvement. *Jpn. J. Appl. Phys.* 55, 021602. doi:10.7567/JJAP.55.021602
- Obiedkov, A. M., Kaverin, B. S., Egorov, V. A., Semenov, N. M., Ketkov, S. Y., Domrachev, G. A., et al. (2012). Macroscopic cylinders on the basis of radial-oriented multi-wall carbon nanotubes. *Lett. Mater.* 2, 152–156. doi:10.22226/2410-3535-2012-3-152-156
- Park, S. J., Kim, J., Chu, M., and Khine, M. (2018). Flexible piezoresistive pressure sensor using wrinkled carbon nanotube thin films for human physiological signals. *Adv. Mater. Technol.* 3, 1–7. doi:10.1002/admt.201700158
- Sun, G., Wang, X., and Chen, P. (2015). Microfiber devices based on carbon materials. *Mater. Today* 18, 215–226. doi:10.1016/j.mattod.2014.12.001
- Tai, Y., and Lubineau, G. (2016). Double-twisted conductive smart threads comprising a homogeneously and a gradient-coated thread for

- multidimensional flexible pressure-sensing devices. *Adv. Funct. Mater.* 26, 4078–4084. doi:10.1002/adfm.201600078
- Wang, C., Xia, K., Wang, H., Liang, X., Yin, Z., and Zhang, Y. (2019). Advanced carbon for flexible and wearable electronics. *Adv. Mater.* 31, 1–37. doi:10.1002/adma.201801072
- Wang, X., Gu, Y., Xiong, Z., Cui, Z., and Zhang, T. (2014). Silk-molded flexible, ultrasensitive, and highly stable electronic skin for monitoring human physiological signals. *Adv. Mater. Weinheim.* 26, 1336–1342. doi:10.1002/adma.201304248
- Zhan, Z., Lin, R., Tran, V. T., An, J., Wei, Y., Du, H., et al. (2017). Paper/carbon nanotube-based wearable pressure sensor for physiological signal acquisition and soft robotic skin. *ACS Appl. Mater. Interfaces* 9, 37921–37928. doi:10.1021/acsami.7b10820
- Zheng, Q., Lee, J. H., Shen, X., Chen, X., and Kim, J. K. (2020). Graphene-based wearable piezoresistive physical sensors. *Mater. Today* 36, 158–179. doi:10.1016/j.mattod.2019.12.004
- Zhuang, Y., Guo, Y., Li, J., Jiang, K., Yu, Y., Zhang, H., et al. (2020). Preparation and laser sintering of a thermoplastic polyurethane carbon nanotube composite-based pressure sensor. *RSC Adv.* 10, 23644–23652. doi:10.1039/d0ra04479b

**Conflict of Interest:** The authors declare that the research was conducted in the absence of any commercial or financial relationships that could be construed as a potential conflict of interest.

Copyright © 2021 Alaferdov, Vilkov, Kaverin, Ob'edkov and Moshkalev. This is an open-access article distributed under the terms of the Creative Commons Attribution License (CC BY). The use, distribution or reproduction in other forums is permitted, provided the original author(s) and the copyright owner(s) are credited and that the original publication in this journal is cited, in accordance with accepted academic practice. No use, distribution or reproduction is permitted which does not comply with these terms.